ELSEVIER

Tectonophysics 344 (2002) 247–259

TECTONOPHYSICS

www.elsevier.com/locate/tecto

Eocene paleomagnetism of the Caucasus (southwest Georgia): oroclinal bending in the Arabian syntaxis

Mikhail L. Bazhenov*, Valentin S. Burtman

Geological Institute, Academy of Sciences of the Russia, Pyzhevsky per. 7, 109017 Moscow, Russia

Received 18 January 2001; accepted 8 August 2001

Abstract

The Caucasus is very important for our understanding of tectonic evolution of the Alpine belt, but only a few reliable paleomagnetic results were reported from this region so far. We studied a collection of more than 300 samples of middle Eocene volcanics and volcano-sedimentary rocks from 10 localities in the Adjaro–Trialet tectonic zone (ATZ) in the western part of the Caucasus. Stepwise thermal demagnetization isolates a characteristic remanent magnetization (ChRM) in 19 sites out of 31 studied. ChRM reversed directions prevail, and a few vectors of normal polarity are antipodal to the reversed ones after tilt correction. The fold test is positive too, and we consider the ChRM primary. Analysis of Tertiary declinations and strikes of Alpine folds in the Adjaro–Trialet zone and the Pontides in Northern Turkey shows a large data scatter; Late Cretaceous data from the same region, however, reveal good correlation between paleomagnetic and structural data. Combining Late Cretaceous and Tertiary data indicates oroclinal bending of the Alpine structures which are locally complicated with different deformation. The overall mean Tertiary inclination is slightly shallower than the reference Eurasian inclination recalculated from one apparent polar wander path (APWP), but agrees with other. This finding is in accord with geological evidence on moderate post-Eocene shortening across the Caucasus. We did not find any indication of long-lived paleomagnetic anomalies, such as to Cenozoic anomalously shallow inclinations further to the east in Central Asia. © 2002 Elsevier Science B.V. All rights reserved.

Keywords: paleomagnetism; Caucasus; oroclinal bending

1. Introduction

Our understanding of tectonic evolution of mobile zones of the Earth greatly benefited from spatial and temporal constraints imposed by paleomagnetic data. It is not surprising that about half of paleomagnetic studies performed worldwide during the last two decades was dedicated to tectonics. The Alpine belt in particular was the target of many works and is by now the most thoroughly investigated fold belt (e.g., Van der Voo, 1993). There are, however, still many areas nearly devoid of paleomagnetic data even this belt. Not only the data density is important; of still larger importance is the quality of the results. Many paleomagnetic data more than a decade old do not satisfy the modern reliability standard anymore; that is why paleomagnetic re-visits of many areas are so common.

The Caucasus occupying the isthmus between the Black and Caspian Seas is just an example. Many

* Corresponding author.
E-mail address: palmag@online.ru (M.L. Bazhenov).

0040-1951/02/$ - see front matter © 2002 Elsevier Science B.V. All rights reserved.
PII: S0040-1951(01)00189-5

studies of Cenozoic and Mesozoic rocks were performed here; enough to say that more than a score of Paleogene paleomagnetic results from different tectonic units of the Caucasus are available. Almost all of them, however, are decades old, are based on very poor cleaning or NRM values and are published only in paleomagnetic databases (e.g., Khramov, 1984). In general, quite a few reliable paleomagnetic data from the Caucasus have been reported up to date.

We had contributed to the Caucasus data set, too; in particular, paleomagnetic data on Eocene rocks from southwest Georgia based on thermal cleaning to not more than 380° and somewhat subjective selection of the results were published (Bazhenov and Burtman, 1990). Here, we would like to present a re-study of this collection from southwest Georgia and to discuss tectonic and geophysical implications of the results.

2. Geological setting and sampling

Tectonic zones of the Alpine belt from the Arabian syntax to the north of the Arabian platform. The syntax consists of several arcuate belts delineated by Cenozoic folds (Burtman, 1989, 1994) and is divided into northern and southern domains by the North Anatolian (NA) strike-slip fault (Fig. 1a). The East Taurides (ET) arc in the southern domain envelopes the northern part of the Arabian platform, while several conjugated arcs are recognized in the northern domain. The concave-south Lesser Caucasus (LC) arc passes into the concave-north Alborz (AL) and Trabzon (TR) arcs to the east and west, respectively (Fig. 1a). The Pont-Caspian fault separates the LC from the Rioni–Shirvan massif that is covered by weakly deformed Cretaceous and Paleogene sediments (Fig. 1b). This massif in turn separates arcuate structures of the Lesser Caucasus from rectilinear structures of the Greater Caucasus (Fig. 1a–b).

The northwestern part of the Lesser Caucasus is occupied by the Adjaro–Trialet tectonic zone (ATZ) (Fig. 1b–c) which comprises a more than 5000-m thick pile of volcanics and volcano-sedimentary rocks. In the west, alkali basalt and tholeiites prevail at the section base and top, whereas the section middle is intercalating basic, alkali intermediate and acid volcanoclastic and tuffaceous rocks with sedimentary interbeds. Eastward, the thickness of the sequence decreases, and calc-alkali volcanics prevail. Nummulites in volcano-sedimentary rocks point to a middle Eocene age of the sequence, but the section top may be of a late Eocene age in the east (Gamkrelidze, 1949; Adamia et al., 1974b; Mrevlishvili, 1974). The ATZ is regarded as an Eocene rift (Adamia et al., 1974a,b; Lordkipanidze, 1980). The Eocene rocks conformably overlie Cretaceous–Paleocene series which outcrop in the cores of some anticlines (Fig. 1c).

Fold axes are of E–W strike in the eastern and central parts of the ATZ and of NE–SW strike in the west (Fig. 1c). Further to the west, the ATZ structures are traced to the East Pontides in Turkey which also comprise of Upper Cretaceous to Eocene volcanic and sedimentary rocks and is thus an extension of the ATZ (Bingol, 1989).

The northern boundary of the ATZ passes along the Surami–Gokishuri Fault (Fig. 1c), which is the western part of the Pont-Caspian fault. This fault is a thrust as evidenced by field observations and borehole data (Basheilishvili et al., 1982; Basheleishvili, 1989; Bazhenov and Burtman, 1990); the magnitude of northward thrusting onto the Rioni–Shirvan massif is about 15 km. The thrust pile about three to 4 km in thickness

Fig. 1. (a) Structural arcs of the Arabian syntax: AL, Alborz arc; ET, East Taurus arc; LC, Lesser Caucasus arc; TR, Trabzon arc. Thin dashed lines are the strikes of Cenozoic folds. Thick toothed lines are major thrusts: PC, Pont-Caspian Fault. Thick solid lines are major strike-slip faults: NA, North Anatolian Fault; small solid arrows denote the sense of displacement. Large open arrows show motion of a point (star) on the Arabian plate with respect to Eurasia for the last 30 My (after Savostin et al., 1986). (b) Schematic tectonic map of the Caucasus region and paleomagnetic sampling localities. MT, Main Thrust of the Great Caucasus, TF—Thrust Front of the southern slope of the Great Caucasus. Solid circles and squares, Late Cretaceous and Paleogene sampling localities, respectively: A, E1–E5—from Bazhenov and Burtman (1989); AD—from Adamia et al. (1979); BS—from Bolshakov and Solodovnikov (1981); C5 and C8 9 from Channell et al. (1996); NA and TB—this paper; TA—from Tatar et al. (1995); V1 and V2—from Van der Voo (1968). Other notation as in panel (a). (c) Structural scheme of the central and western parts of the Adjaro Trialet zone (white) and paleomagnetic sampling localities (open rectangles); localities NA and TB in the eastern part of the zone are shown in panel (b). Thick solid lines are the axes of anticline folds. Thick dashed line is the Surami–Gokishuri Thrust.

is divided into several sheets. The youngest rocks in the footwall of the thrust are of late Miocene to Pliocene age. The hanging wall of the thrust is gently folded, whereas the folds are much tighter further to the south in other parts of the Adjaro–Trialet zone. Judging from these facts folding is likely to have taken place after, or synchronously with, thrusting. The Pliocene age of deformation is confirmed by angular unconformity

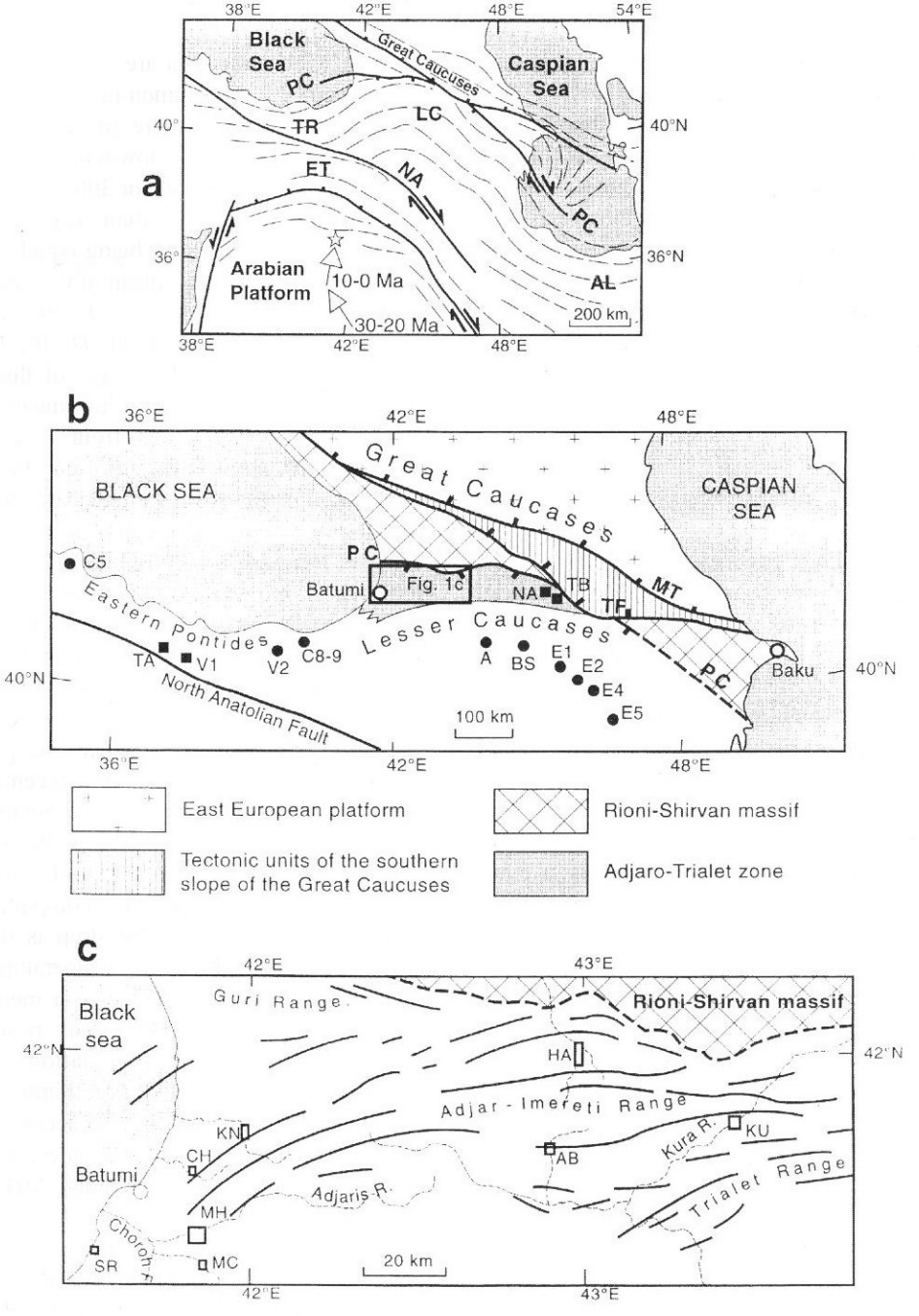

between folded lower Pliocene and weakly deformed upper Pliocene strata in the eastern part of the Adjaro–Trialet zone.

We sampled middle Eocene volcanics and volcanosedimentary rocks from 10 localities (31 sites) from different parts of the zone (Fig. 1b–c). The study area has subtropical humid climate, and all mountains are covered by thick vegetation. Hence, the number and dimensions of outcrops are limited, and many exposures of volcanics were rejected because of the lack of stratification. As a result, basalt flows could only be sampled from locality SR. The true thickness studied at each site varies from several meters to several tens of meters. One hand-sample oriented with a magnetic compass was taken at each stratigraphic level, samples being spaced more or less uniformly across the sampled outcrops. In total, more than 300 hand samples of mostly tuffaceous sandstones and siltstones were taken.

3. Methods

One cubic specimen from each hand-sample was subjected to progressive thermal demagnetization in 12–18 steps up to 610 °C in a home-made oven with internal residual fields of about 10 nT and measured with a JR-4 spinner magnetometer with a noise level of 0.05 mA/m. Basalt samples from site SR1 were also subjected to alternating fields up to 80 mT in a home-made device. Demagnetization results were plotted on orthogonal vector diagrams (Zijderveld, 1967), and directions of magnetic components and orientation of remagnetization circles were determined by a least squares fit comprising three measurements or more (Kirschvink, 1980). The characteristic remanent magnetization (ChRM) was determined without anchoring the final linear segments to the origin of the vector diagrams. Paleomagnetic software for IBM PC by Randy Enkin and Stanislav Shipunov and for Macintosh by Jean-Pascal Cogné was used for analysis.

4. Results

NRM intensities in tuffaceous sediments vary from nearly 1 to 0.01 A/m. No correlation was found between the NRM intensity and demagnetization characteristics or component directions, whereas distinct correlation was observed between the NRM drop after heating to 100° or 200° and the quality of demagnetization data. A well-defined ChRM was easily isolated above 250° or 300° from samples where this drop is less than, or comparable to, a more stable part of NRM (Fig. 2a–b).

Demagnetization data are more noisy, and several linear segments are common in the samples where the NRM initial drop is more prominent (Fig. 2c–e). Site-mean directions of a low-temperature component isolated from 100° to 250° or 300° (Fig. 2e) are much better clustered in situ than after tilt correction, concentration parameter k being equal to 104 and 4, respectively. The overall mean of the low-temperature component in situ ($D=11°$, $I=59°$, $a_{95}=5.5°$) is close to the present-day field ($D=0°$, $I=61°$), indicating a recent post-folding age of this remanence. Components corresponding to linear segments at intermediate temperatures from 200° or 250° to 400° to 450°, sometimes 500°, are very scattered in both coordinates. Also scattered are directions of a high-temperature component in multi-component samples (Fig. 2d–e). In addition, no consistent pattern was found in many samples after initial sharp drop in NRM intensity; because of this, several sites from localities MH, and MC, all but one site from locality KIN, and all sites from locality TB were discarded.

We think that two components are present in this rocks. The first component is a recent post-folding overprint of ubiquitously normal polarity. The second component is the ChRM in the samples with small initial NRM drop. High dispersal of intermediate-and high-temperature components in samples with large initial NRM drop is due to strong overlapping of unblocking temperature spectra of the overprint and ChRM; hence a method of combining direct observations and remagnetization circles was used for computation of site-mean directions (McFadden and McElhinny, 1988). Even with the aid of this method, no acceptable grouping of direct observations and remagnetization circles is achieved at sites MC2, MH4 and MH6, which are rejected.

NRM intensities in basalt samples from sites SR1 are above 10 A/m. Both thermal and alternating field demagnetization revealed a well-defined ChRM in

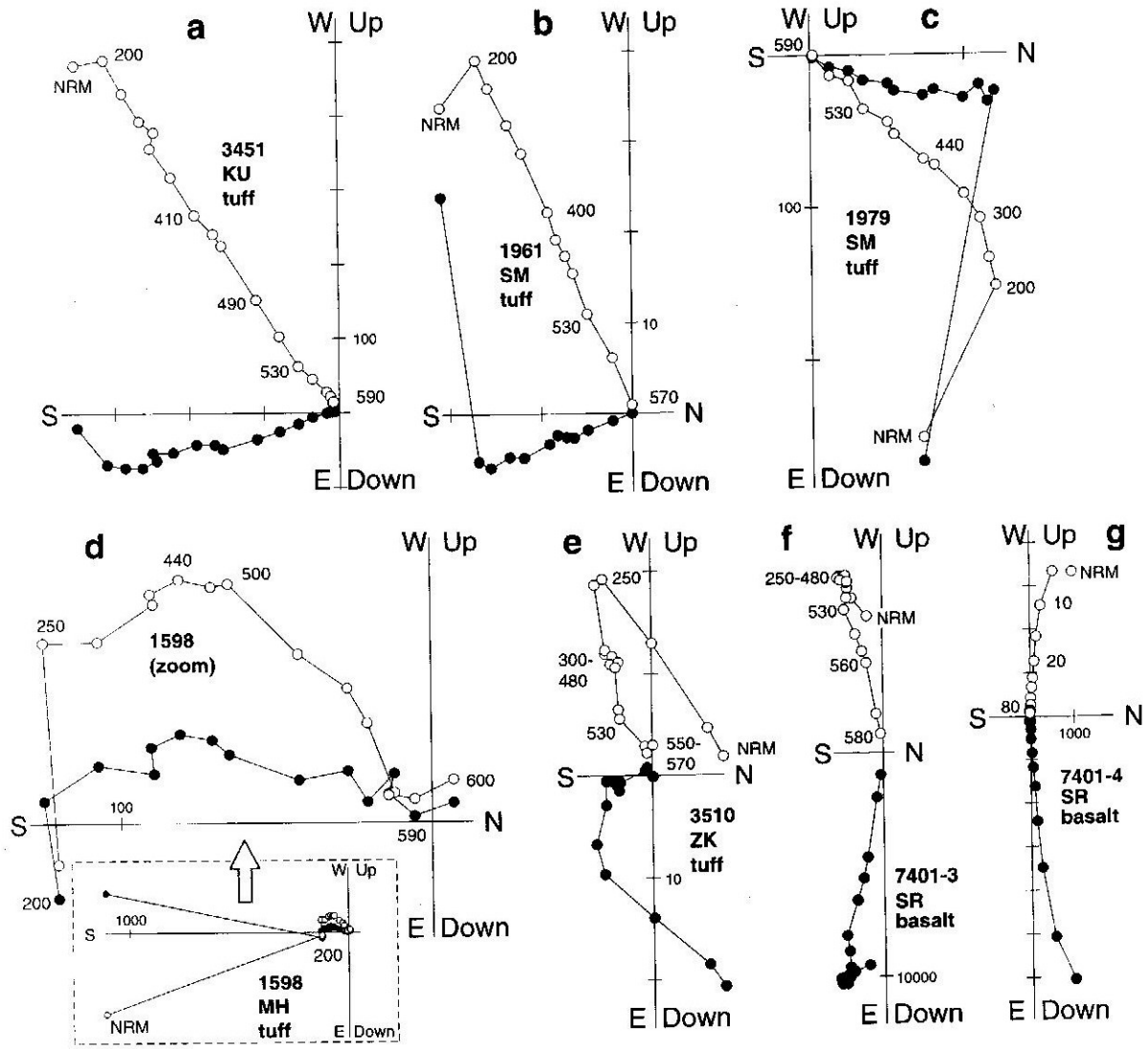

Fig. 2. Representative thermal (a–f) and alternating field (g) demagnetization plots of Eocene rocks from the Adjaro–Trialet zone in stratigraphic coordinates. Full (open) dots represent vector endpoints projected onto the horizontal (vertical) plane. Temperatures are in °Celsius; alternating fields are in millitesias. Magnetization intensities are in mA/m.

some samples (Fig. 2f–g), while other basalt samples gave no consistent results above 250° to 300° and were discarded.

Sampling localities are distributed over an area about 300 km in length, i.e., less than 3° of great circle (Fig. 1b–c), and variance in declination between locality means is not large. For the most separated localities NA and SR, the "recalculation errors" (Van der Voo, 1993) do not exceed 1° either in declination or inclination and are thus negligible. So all paleomagnetic directions were combined as they are for further analysis.

Nineteen site-mean directions from nine localities are much better clustered after tilt correction than in situ (Fig. 3; Table 1). At the same time, some smearing of the tilt-corrected data is evident (Fig. 3b), and a

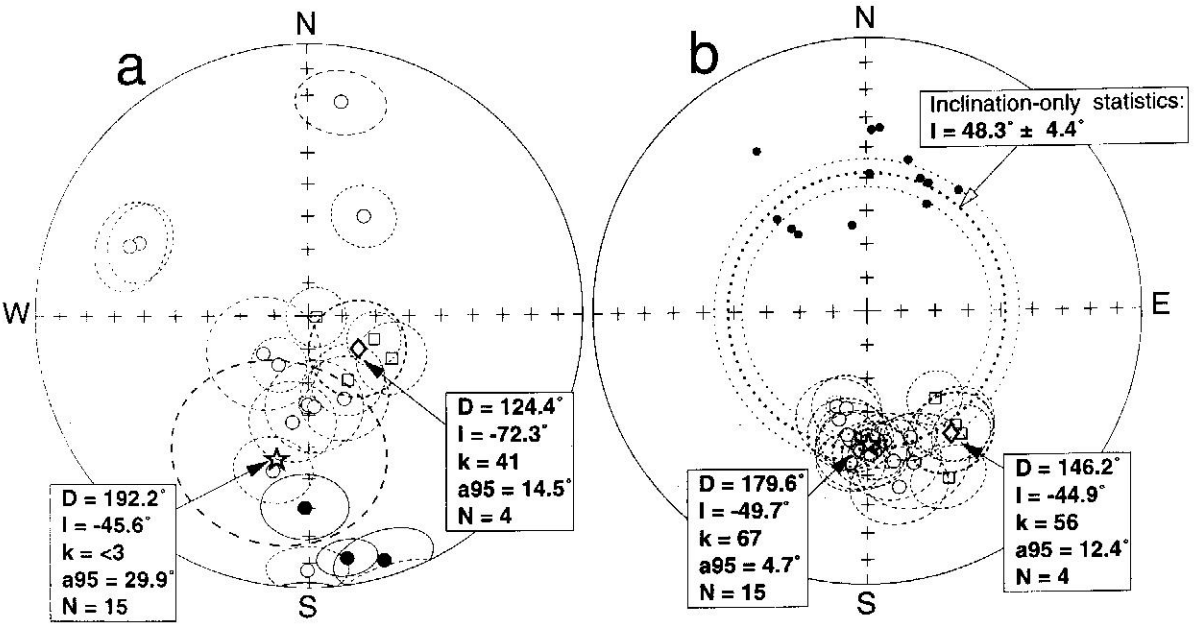

Fig. 3. Equal-area projection of site-mean ChRM directions (dots) (a b) together with associated confidence circles (thin lines) in situ (a) and after tilt correction (b). Small solid dots in (b) are unit ChRM directions from sites NA2, KN3 and MH5. Star and diamond are overall means with associated confidence circles (thick dashed line) for the main data set and the site with northwestern declinations, respectively (see text for explanations). Thick and thin dotted lines are mean inclinations obtained by the inclination-only statistics and their confidence limits, respectively. Open (solid) symbols and dashed and dotted (solid) lines are projected onto upper (lower) hemisphere.

closer inspection reveals that two localities from the southwestern part of the ATZ (MC and SR) yield more westerly declinations than the main data set. While mean inclinations of these two groups differ by just $4.8 \pm 10.6°$, the difference in declination of $33.4 \pm 15.2°$ is statistically significant (Table 1). The fold test is positive for the main set of 15 sites, and the best data grouping is achieved after tilt correction. The fold test for four sites with westerly declinations is inconclusive because of similar bedding attitudes. Mean inclination was calculated for the entire data set with the aid of inclination-only statistics at the site-mean level (McFadden and Reid, 1982); the inclination-only fold test is positive for the entire set.

After tilt correction, almost all ChRM directions are reversed; few normally magnetized samples from sites NA2, KN3, and MH5 are antipodal to reversed site-means (Fig. 3b). The presence of two polarities and the positive fold test indicate that the remanence of the rocks studied is likely to be primary. Geological data indicate middle Eocene age for the volcanic series (Adamia et al., 1974b; Mrevlishvili, 1974), and the ChRM is likely to be 43 ± 6 Ma old.

5. Analysis of declination data

Paleomagnetic declinations are analyzed with the aid of plots of declination vs. strike of folds (D–S plots). On such plots, a regression line parallel to the strike axis corresponds to originally curved structure (no rotations), while a line inclined at 45° to the same axis stands for oroclinal bending of an originally rectilinear structure. Paleomagnetic directions together with confidence limits for declination are taken from this study and published data; our data were used at the locality-mean level. The strikes of folds are read from detailed geological maps, and the error bars of $\pm 5°$ are assigned to all strike values.

Table 1
Site-mean and locality-mean paleomagnetic results for ChRM

S&L	Data	N	B	In situ				TILT-corrected			
				D°	I°	k	a_{95}°	D°	I°	k	a_{95}°
NA1	m	18/14	168/46	180.4	−7.0	20	9.2	187.9	−51.0	23	8.6
NA2	m	15/9	185/77	188.0	24.7	22	11.4	189.3	−52.4	22	11.2
NA		33/23		183.6	6.3	12	9.1	188.6	−51.6	24	6.3
HA1	m	12/12	11/21	157.1	−62.8	13	12.8	170.2	−43.7	13	12.8
HA2	m	13/10	16/80	29.1	55.7	28	9.4	186.4	−43.7	28	9.4
HA		25/22		88.6	75.5	6	12.3	177.7	−44.0	13	8.1
AB1	f	12/11	341/28	176.5	−62.5	11	14.1	169.9	−35.0	14	12.9
AB2	f	12/12	222/12	192.9	−41.2	17	10.8	185.8	−51.6	17	10.8
AB		24/23		187.0	−51.7	12	8.3	177.1	−44.0	13	8.1
KU	f	18/11	191/78	181.2	30.1	17	11.3	178.7	−46.5	20	10.5
CH1	f	13/7	322/77	291.6	−30.7	26	12.0	194.8	−56.6	25	12.3
CH2	f	14/13	321/73	293.6	−33.4	16	10.7	192.2	−60.3	18	10.0
CH		27/20		292.7	−32.5	21	6.9	193.2	−59.0	21	6.9
KN3	f	15/6	319/46	229.6	−72.4	16	17.0	163.2	−41.6	20	15.3
MH1	m	9/6	147/60	163.1	6.7	44	11.4	172.6	−50.3	76	8.6
MH2	m	14/12	158/60	171.1	10.7	44	7.0	177.2	−47.4	27	8.9
MH3	m	15/11	315/33	210.9	−72.9	34	8.2	161.5	−49.8	42	7.5
MH5	m	9/7	341/11	188.6	−57.4	28	12.4	182.8	−47.7	27	12.6
MH7	f	14/14	82/10	180.5	−63.2	208	2.8	197.9	−60.2	162	3.1
MH		61/50		177.6	−41.0	4	9.4	178.6	−52.6	29	3.7
MAIN		(15)		192.2	−45.6	<3	29.9	179.6	−49.7	67	4.7
MC1	m	7/6	339/35	149.0	−67.4	43	10.8	154.3	−32.8	48	10.1
MC3	f	11/8	325/45	100.2	−87.6	40	8.9	143.0	−43.0	44	8.4
MC		18/14		143.7	−79.3	27	7.2	148.2	−38.8	36	6.2
SR1	m	9/9	0/23	117.6	−62.0	25	10.6	142.7	−46.4	22	11.2
SR2	f	9/5	0/20	110.2	−69.3	90	8.1	142.7	−56.9	90	8.1
SR		18/14		152.9	−31.6	27	7.3	142.7	−50.2	28	7.0
DEV		(4)		124.4	−72.3	41	14.5	146.2	−44.9	56	12.4
INC		(19)			−48.5		17.2		−48.3		4.4

S&L, sites and localities; localities are labeled as in the text and Fig. 1 (locality TB is not included as no meaningful results was obtain here); MAIN and DEV, mean directions for the main group of sites and sites with deviating northwesterly declinations from localities MC and SR, respectively (see text for explanation).

INC, inclination-only statistics (McFadden and Reid, 1982). Data, the type of data used (for site-means only): f, mean vector for direct observations (Fisher, 1953), m, mixed direct observations and remagnetizations circles (McFadden and McElhinny, 1988). *N*, number of samples studied/accepted (only samples from the sites which gave acceptable date are included); number of sites is in brackets. *B*, azimuth of dip/dip angle; *D*, declination; *I*, inclination; *k*, precision parameter (Fisher, 1953); a_{95}, radius of confidence circle. All locality-means are calculated at the sample-mean level.

The *D*–*S* plots of Paleogene data shows large scatter of the data from the ATZ (Fig. 4a). One can either exclude entries CH, KN and MH and conclude that the ATZ is an orocline; alternatively, exclusion of entries SR and MC indicates an originally curved structure with non-systematic local rotations of both senses.

We attempted to reinforce our analysis by other Tertiary and Late Cretaceous data from the Lesser Caucasus and Pontides. Such an extension of the area under consideration is justified by the fact that the present-day tectonic pattern in the Pontides and Lesser Caucasus was formed during major deformation of late Cenozoic age. Further justification is the similarity of Tertiary and Late Cretaceous Eurasian expected declinations for this region (Besse and Courtillot, 1991; Van der Voo, 1993). These two observations allow us to combine Tertiary and Late Cretaceous paleomagnetic results to the north of the North Anatolian Fault for analysis of rotations. A brief overview of published data, however, is required.

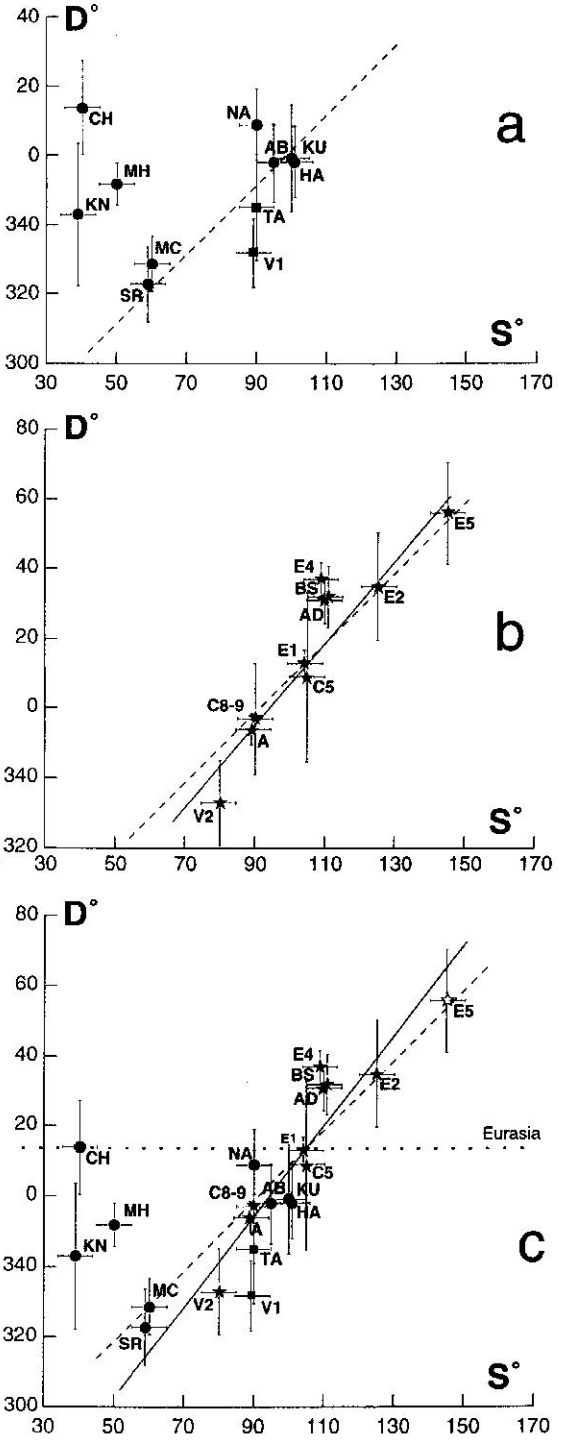

Everywhere, we excluded all results based on inadequate statistics; in particular, Tertiary and Late Cretaceous results based on just two or three sites from the Pontides were excluded because adequate averaging of secular variation is not achieved in these cases. Also excluded were the results from structurally disturbed areas and those whose structural settings cannot be determined. Most results from the Lesser Caucasus are based on very poor demagnetization (Khramov, 1984) and do not merit further consideration. Paleomagnetic directions obtained during paleointensity studies of Armenian Paleogene volcanics are based on thermally demagnetized data (Solodovnikov, 1998, 1999); all data, however, are in situ, and no information for tilt-correction is provided thus precluding the use of these data, too. Pechersky and Nguen (1978) reported moderately well demagnetized data from a limited part of the Lesser Caucasus which show a clear banana-type distribution. This distribution is likely to have resulted from local rotations (MacDonald, 1980), and the use of these results for our regional analysis is not justified. Adamia et al. (1979) and Bazhenov and Burtman (1989) reported Late Cretaceous data based on cleaning up to 500° and confirmed by positive fold and reversal tests; despite incomplete demagnetization, these results are used (A, AD, E1–E5; Fig. 1b). Also used is the result (BS; Fig. 1b) obtained during paleointensity studies (Bolshakov and Solodovnikov, 1981). From the Eastern Pontides, two Paleogene results, V1 of Van der Voo (1968) and TA of Tatar et al. (1995), and three Late Cretaceous data, V2, C5 and C8–9 from (Van der Voo, 1968; Channell et al., 1996) were used.

The addition of Paleogene results (V1 and TA) from the Pontides to the declination-vs.-strike plot does not make the pattern clearer (Fig. 4a). In contrast, the linear regression for the Late Cretaceous data is

Fig. 4. Plots of declination D vs. strike of folds S for Paleogene (a), Late Cretaceous (b) and combined (c) data together with the error limits for the both variables. Dots, our data; squares, published results (see Fig. 1a–b for location of sampled areas): AD, Adamia et al. (1979); A and E1 to E5, Bazhenov and Burtman (1989); BS Bolshakov and Solodovnikov (1981); C – 5 and C8 + 9, group-means from Channell et al. (1996); TA, Tatar et al. (1995); V1 and V2, Van der Voo (1968). Solid and dashed lines are calculated regressions and theoretical plots for originally rectilinear structure, respectively. Thick dotted lines denote expected declinations for the study area (see text).

very close to the theoretical line for an orocline with the moderate data scatter (Fig. 4b). Late Cenozoic age of major deformation in the Lesser Caucasus and the Pontides allow us to pool the data. After pooling, oroclinal bending of the Lesser Caucasus and Pontides becomes evident (Fig. 4c). Also clear is that the results from localities CH, KN and MH are anomalous. These three results from the northwestern part of the ATZ are from structures of NE–SW strike, similarly with results from localities SR and MC (Fig. 1c). The KN result is poorly defined, while the CH and especially MH are of better quality. Very important is that the CH, KN and MH mean directions agree with the other data from the central and eastern parts of the ATZ (Fig. 3b; Table 1), and their anomalous position on the $D-S$ plot cannot be blamed on paleomagnetic reasons. We conclude that these structures of similar strike have divergent paleomagnetic directions and, therefore, regional oroclinal bending of the Pontides and Lesser Caucasus is locally complicated by deformation of different type(s).

Note that the regression is somewhat steeper than the theoretical line for an originally rectilinear structure (Fig. 4c). The statistical significance of this difference is difficult to evaluate, and it may be due to random errors. We cannot, however, exclude a possibility that the Lesser Caucasus–Pontides arc had originally been slightly curved in the opposite direction.

During oroclinal bending all parts of a structure rotate through different angles except for a limited translated part provided that there is no net rotation of the entire structure. (There is no geological data which indicate a rotation of the Lesser Caucasus–Pontides arc as the whole, and we do not consider this case anymore.) On the $D-S$ plot, the translated segment can be found as an intersection of the regression line with the reference declination (Fig. 4c). The latter are similar in

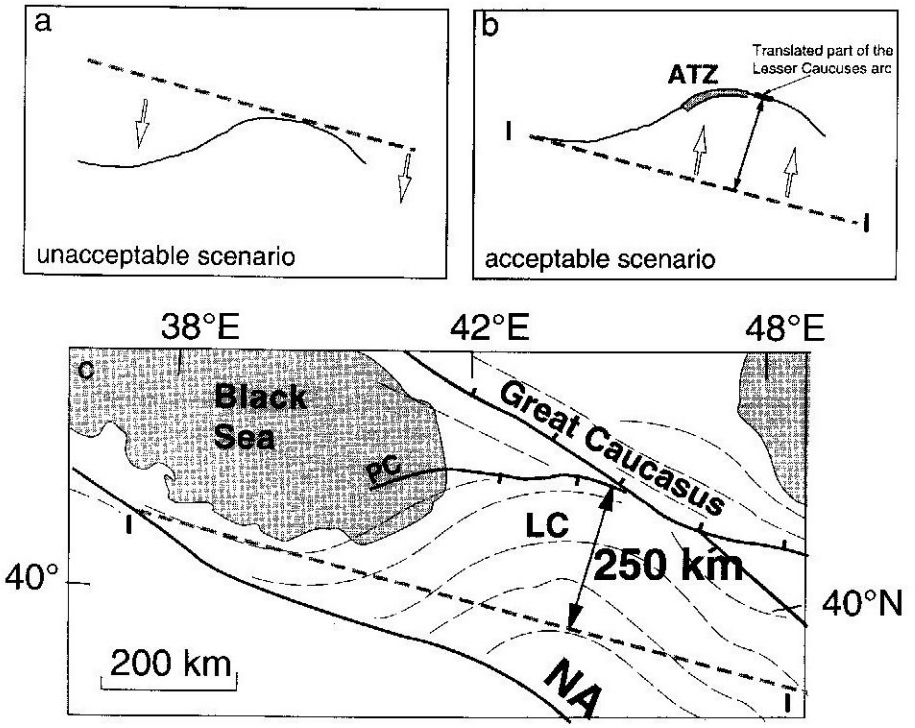

Fig. 5. (a–b) Cartoons illustrating oroclinal bending of the Lesser Caucasus arc: (a) unacceptable scenario; (b) acceptable scenario. Thin solid line is the present-day arc. Thick dashed line is this arc before bending assuming no general northward translation (see text). Open arrows denote landmasses motion on the limbs of the orocline. Solid double-pointed arrow is the maximum displacement. (c). Application of the scenario (b) to the Lesser Caucasus. Dashed line (I–I) corresponds to original position and orientation of the arc without its displacement. Other notation as in Figs. 1a and (b).

the Eurasian frame for both APWPs used, and hence the non-rotated part of the Lesser Caucasus–Pontides arc has strikes of about 100–110° (Fig. 4c). Thus, it had originally been a rectilinear or slightly northward concave structure of nearly E–W strike.

The convergence of the Eurasian and African plates was generally in a south-to-north direction (Savostin et al., 1986; Van der Voo, 1993). Hence, any part of the arc could hardly move southward (Fig. 5a); instead, northward motion of landmasses is strongly indicated by all available data (Fig. 5b) A schematic reconstruction of oroclinal bending (Fig. 5c) allows us to evaluate the magnitude of displacement along the Lesser Caucasus–Pontides arc. This displacement amounts to about 250 km in the central part of the arc assuming an originally rectilinear form (line I–I in Fig. 5b–c). As the ATZ is close to the arc apex, its displacement was similar to the above value. It should be stressed that this value of displacement is the lower limit as the entire structure could move as the whole; we cannot, however, estimate the general displacement from available data.

6. Analysis of inclination data

An apparent polar wander path (APWP) of a plate can be constructed either using paleomagnetic poles only from this plate (e.g., Van der Voo, 1993), or combining coeval data from all continents restored to their correct positions with the aid of plate kinematics (Besse and Courtillot, 1991). Note that the APWPs derived by each method show general and disagree in detail. Each approach has its pros and cons, and we would not like to delve into an analysis here. We simply compare our results with the two APWPs for the Eurasian and African plates from the above cited publications. All reference directions were calculated for a common point at 41.8°N, 42.5°E. The 40- and 50-Ma mean poles from the master APWP of Besse and Courtillot (1991) were interpolated to obtain the 45-Ma mean pole.

The African and Eurasian Tertiary expected inclinations agree recalculated from the APWP of Van der Voo (1993), and the F value of $4.0 \pm 5.0°$ is statistically insignificant with respect to the Eurasian direction. In contrast, the reference inclination plots for Eurasia and Africa (Besse and Courtillot, 1991) steadily diverge with time (Fig. 6a). The observed Eocene inclination of $48.3 \pm 4.4°$ is significantly shallower than the Eurasian direction and closely matches the African one; the values of flattening $F = I_{exp} - I_{obs}$, where subscripts exp and obs refer to expected and observed values, respectively, are $9.7 \pm 5.0°$ and $3.0 \pm 5.0°$, respectively. Thus, definite conclusions cannot be reached because of inconsistency of reference data.

At the same time, the measured inclination is somewhat lower than all reference data. There are three reasons why the observed inclination from the ATZ may be shallower than the Eurasian reference value: (i) most results are derived from sediments, and inclination shallowing may bias the mean inclination; (ii) the study area belongs to the Alpine fold belt, and all geologic data from the Caucasus region indicate northward transport of land masses during Cenozoic defor-

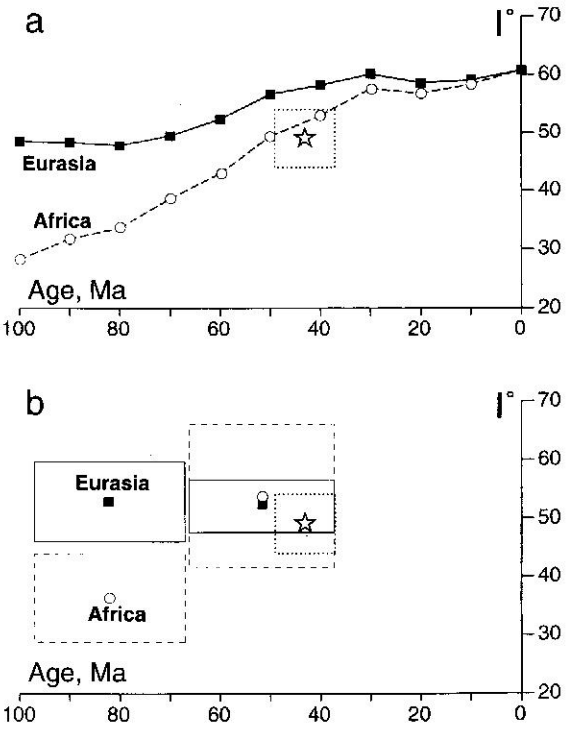

Fig. 6. Plots of inclination $I°$ vs. age for the overall mean of the ChRM from the Adjaro–Trialet zone (star) with confidence limits and the reference data for the African (open circles) and Eurasian (solid squares) plates from (a) Besse and Courtillot (1991) and (b) Van der Voo (1993). In panel (b), error limits are shown as solid and dashed lines for the Eurasian and African data, respectively.

mation of the region (Savostin et al., 1986; Van der Voo, 1993); (iii) systematically low Cenozoic inclinations were observed in mid-northern latitudes of the northern hemisphere (Westphal et al., 1986), the origin of this Cenozoic inclination anomaly (CIA), being unknown. The problem is how these three sources of inclination shallowing are partitioned in our case.

No anisotropy measurements could be performed due to the lack of unheated samples. Note, however, that the mean inclination of 46.4° from the only basalt site studied (SR1) is close to the overall mean inclination of 48.3° (Table 1, Fig. 3b). Thus, there is no reason to suspect large inclination shallowing in our data.

The convergence of the Eurasian and African plates was generally to the north in the late Cenozoic (e.g., Savostin et al., 1986). In the Caucasian region, the last ocean was closed in the Cenomanian–Coniacian (Knipper, 1975), and the northward displacement of the study area could only have been accommodated by deformation of the continental crust. In the previous chapter, it was shown that the Late Cretaceous and Paleogene paleomagnetic data from the Lesser Caucasus indicate an oroclinal bending of the entire belt which took place in post-Eocene time. From dimensions of the bent structures, the amount of northward displacement of the arc apex cannot be less than 250 km (Fig. 5b–c).

Unwrapping of alpine folds of the Great Caucasus indicate shortening of about 80–120 km (Dotduev, 1986). Metamorphic rocks of this range are thrust about 20 km southward over the Flysch Zone and other tectonic units of southern slope of the Great Caucasus along the Main Great Caucasus Thrust (Fig. 1b). In turn, the Flysch Zone is cut by numerous thrusts of southern vergence and, as the whole, is thrust over the Rioni–Shirvan massif (Gamkrelidze and Gamkrelidze, 1977; Dotduev, 1986); the shortening of this zone is about 60 km The total shortening across the Great Caucasus is at least 200 km and probably more, as evidenced by sharp contrasts between Jurassic formations in the different tectonic units of this range and the Rioni–Shirvan massif (Dotduev, 1989; Bazhenov and Burtman, 1990). Moreover, tectonic units of the Great Caucasus completely overlap the central part of the Rioni–Shirvan massif, whose width to the east and west is more than 100 km, and the eastern part of the ATZ (Fig. 1b) (Krasovsky et al., 1990). Northward thrusting of about 15 km was established along the northern margin of the ATZ (Basheilishvili et al., 1982; Basheleishvili, 1989); folding in the ATZ contributed to shortening, too.

Taken together, geological data and unbending of the Lesser Caucasus–Pontides arc indicate shortening of at least 400 km in the Caucasus region. It should be stressed that this value is the lower limit of convergence, and its true magnitude may be larger. This estimate of shortening corresponds to an inclination difference of about 5°. Subtracting this value makes the F parameter insignificant for the both APWPs (Besse and Courtillot, 1991; Van der Voo, 1993). Hence, the sum of inclination shallowing and CIA becomes insignificant, too.

Anomalously low Tertiary inclinations were reported from the central Mediterranean to Turkey and Iran to the Pamirs (Westphal et al., 1986; Westphal, 1993); similar results were reported from China, too (Huang and Opdyke, 1992; Gilder et al., 1996; Cogne et al., 1999). The origin of this phenomenon remains enigmatic despite quite a number of disparate hypotheses suggested (see Cogne et al., 1999, for review). The Lesser Caucasus falls into the CIA too, and, according to a general CIA map (Chauvin et al., 1996), its magnitude of about 10° may be expected here. We showed, however, that this anomaly should be less than 5° that is within the error limits of available data. Taking into account that we could determine only the minimal shortening and a possibility of inclination shallowing leaves no "room" for the CIA. Therefore, in contrast to Central Asia, no considerable inclination anomaly exists in the Caucasus.

Acknowledgements

We thank Natalia Levashova for her helpful comments on a draft of the paper and Rob Van der Voo and Michel Westphal for instructive reviews. This study was supported by grant no. 00-55-64148 from the Russian Foundation for Basic Research.

References

Adamia, Sh.A., Gamkrelidze, I.P., Zakariadze, G.S., Lordkipanidze, M.B., 1974a. The position of the Adjaro–Trialet zone in the Alpine belt. In: Gamkrelidze, I.P., Rubinstein, M.M. (Eds.),

Problems in Geology of Adjaro–Trialetia. Metsniereba, Tbilisi, pp. 155–171 (in Russian).

Adamia, Sh.A., Zakariadze, G.S., Lordkipanidze, M.B., Sulukvadze, N.Sh., 1974b. Geology of Adjaria. In: Gamkrelidze, I.P., Rubinstein, M.M. (Eds.), Problems in Geology of Adjaro–Trialetia. Metsniereba, Tbilisi, pp. 60–69 (in Russia).

Adamia, Sh.A., Asanidze, B.Z., Gambashidze, R.A. Nadareishvili, G.Sh., Nguen, T.K.T., Pechersky, D.M., 1979. Paleomagnetism of Upper Cretaceous rocks from Southern Georgia and its geological interpretation. Izv. Akad. Nauk SSSR, Ser. Geol. 5, 46–57 (in Russia).

Basheilishvili, L.B., Burtman, V.S., Gamkrelidze, I.P., 1982. The boundary zone between the Adjaro–Trialet fold zone and the Dzirula massif. Dokl. Akad. Nauk SSSR 266, 196–198 (in Russian).

Basheilishvili, L.V., 1989. Tectonics of the contact zone between the Adjaro–Trailet folded zone and the Georgian block. Geotectonics 23, 367–375.

Bazhenov, M.L., Burtman, V.S., 1989. Paleomagnetism of Upper Cretaceous rocks from the Caucasus and its implications for tectonics. In: Sengor, A.M.C. (Ed.), Tectonic Evolution of the Tethyan Region. Kluwer Academic Publishing, Dordrecht, pp. 217–239.

Bazhenov, M.L., Burtman, V.S., 1990. The Structural Arcs of the Alpine Belt (The Carpathians, Caucasus, Pamirs). Nauka, Moscow, 168 pp. (in Russian).

Besse, J., Courtillot, V., 1991. Revised and synthetic polar wander paths of the African, Eurasian, North American and Indian Plates, and true polar wander since 200 Ma. J. Geophys. Res. 96, 4029–4050.

Bingol, E., 1989. Geological Map of Turkey in Scale 1:2,000,000. MTA, Ankara.

Bolshakov, A.S., Solodovnikov, G.M., 1981. Intensity of the geomagnetic field in the Late Cretaceous. Izv. Akad. Nauk SSSR, Ser. Fiz. Zemli 10, 58–68 (in Russian).

Burtman, V.S., 1989. Kinematics of the Arabian syntaxis. Geotectonics 23, 139–145.

Burtman, V.S., 1994. Meso-Tethyan oceanic sutures and their deformation. Tectonophysics 234, 305–327.

Channell, J.E.T., Tuysuz, O., Bektas, O., Sengor, A.M.C., 1996. Jurrasic–Cretaceous paleomagnetism and paleogeography of the Pontides (Turkey). Tectonics 15 (1), 201–212.

Chauvin, A., Perroud, H., Bazhenov, M.L., 1996. Anomalous low paleomagnetic inclinations from Oligocene–Lower Miocene red beds of the South-West Tien Shan, Central Asia. Geophys. J. Int. 126, 303–313.

Cogne, J.-P., Halim, N., Chen, Y., Courtillot, V., 1999. Resolving the problem of shallow magnetizations of Tertiary age in Asia: insights from paleomagnetic data from the Quangtang, Kunlun, and Qaidam blocks (Tibet, China), and a new hypothesis. J. Geophys. Res. 104, 17715–17734.

Dotduev, S.I., 1986. The nappes of the Great Caucasus. Geotektonika 5, 94–106 (in Russian).

Dotduev, S.I., 1989. Mesozoic and Cenezoic geodynamics of the Great Caucasus. In: Belov, A.A., Satian, M.A. (Eds.), Geodynamic of the Caucasus. Nauka, Moscow, pp. 82–92 (in Russian).

Fisher, R.A., 1953. Dispersion on a sphere. Proc. R. Soc. London, Ser. A. 217, 295–305.

Gamkrelidze, P.D., 1949. Geological structure of the Adjaro–Trialet fold system. Akad. Nauk GSSR, Tbilisi, 508 pp. (in Russian).

Gamkrelidze, P.D., Gamkrelidze, I.P., 1977. The nappes of the southern slope of the Great Caucasus. Metsniereba, Tbilisi, 82 pp. (in Russian).

Gilder, S.A., Zhao, X., Coe, R.S., Meng, Z., Courtillot, V., Besse, J., 1996. Paleomagnetism and tectonics of the southern Tarim basin, northwest China. J. Geophys. Res. 101, 22015–22032.

Huang, K., Opdyke, N.D., 1992. Paleomagnetism of Cretaceous to lower Tertiary rocks from southwestern Sichuan: a revisit. Earth Planet. Sci. Lett. 112, 29–40.

Khramov, A.N. (Ed.), 1984. Paleomagnetic Directions and Pole 591 Positions (data for the USSR): Summary Catalogue 1. Akad. Nauk SSSR, Moscow, 94 pp. (in Russian).

Kirschvink, J.L., 1980. The least-square line and plane and the analysis of the paleomagnetic data. Geophys. J. R. Astron. Soc. 62, 699–718.

Knipper, A.L., 1975. Oceanic Crust in the Alpine Fold Belt. Nauka, Moscow, 208 pp. (in Russian).

Krasovsky, A.M., Usanov, G.M., Papava, D.Y., Shengelia, M.I., Ebralidze, T.P., Gudushuauri, S.V., 1990. The structure and oil potential of underthrust zones of East Georgia. In: Khain, V.E., Sokolov, B.A., Mirasanova, N.V. (Eds.), Tectonics and Oil Potential of Underthrust Zones. Nauka, Moscow, pp. 78–87 (in Russian).

Lordkipanidze, M.B., 1980. Alpine volcanism and geodynamics of the central segment of the Mediterranean fold belt. Metsniereba, Tbilisi, 162 pp. (in Russian).

MacDonald, W.D., 1980. Net tectonic rotation, apparent tectonic rotation and the structural tilt correction in the paleomagnetic studies. J. Geophys. Res. 85, 3659–3669.

McFadden, P.L., McElhinny, M.W., 1988. The combined analysis of remagnetization circles and direct observations in palcomagnetism. Earth Planet. Sci. Lett. 87, 161–172.

McFadden, P.L., Reid, A.B., 1982. Analysis of paleomagnetic inclination data. Geophys. J. R. Astron. Soc. 69, 307–319.

Mrevlishvili, I.I., 1974. Nummulite zones in middle Eocene of Adjaro–Trialetia. In: Gamkrelidze, I.P., Rubinstein, M.M. (Eds.), Problems in Geology of Adjaro–Trialetia. Metsniereba, Tbilisi, pp. 15–24 (in Russian).

Pechersky, D.M., Nguen, T.K.T., 1978. Paleomagnetism of volcanic rocks from ophiolites and Late Cretaceous extrusives from Armenia. Izv. Akad. Nauk SSSR, Ser. Fiz. Zemli 3, 48–63 (in Russian).

Savostin, L.A., Sibuet, J.C., Zonenshain, L.P., Le Pichon, X., Roulet, M.J., 1986. Kinematic evolution of the Tethys belt from the Atlantic ocean to the Pamirs since the Triassic. Tectonophysics 123, 1–35.

Solodovnikov, G.M., 1998. Intensity of geomagnetic field in the Eocene. Fiz. Zemli 10, 84–88 (in Russian).

Solodovnikov, G.M., 1999. Intensity of geomagnetic field derived from Oligocene and Miocene rocks. Fiz. Zemli 4, 85–90 (in Russian).

Tatar, O., Piper, J.D.A., Park, R.G., Gursoy, H., 1995. Paleomagnetic study of block rotations in the Niksar overlap region of the

North Anatolian Fault zone, central Turkey. Tectonophysics 244, 251–266.

Van der Voo, R., 1968. Jurassic, Cretaceous and Eocene pole positions from northeastern Turkey. Tectonophysics 6, 251–269.

Van der Voo, R., 1993. Paleomagnetism of the Atlantic, Tethys and Iapetus Oceans. Cambridge Univ. Press, New York, 411 pp.

Westphal, M., 1993. Did a large departure from the geocentric axial dipole hypothesis occur during the Eocene? Evidence from the magnetic polar wander path of Eurasia. Earth Planet. Sci. Lett. 117, 15–28.

Westphal, M., Bazhenov, M.L., Lauer, J.P., Pechersky, D.M., Sibuet, J.C., 1986. Paleomagnetic implications on the evolution of the Tethys belt from the Atlantic ocean to the Pamirs from the Triassic. Tectonophysics 123, 37–82.

Zijderveld, J.D.A., 1967. AC demagnetization of rocks: analysis of results. In: Collinson, D.W., Creer, K.M. (Eds.), Methods in Paleomagnetism. Elsevier, Amsterdam, pp. 254–286.